

# Improved Rear-Side Passivation by Atomic Layer Deposition $\text{Al}_2\text{O}_3/\text{SiN}_x$ Stack Layers for High $V_{\text{OC}}$ Industrial $p$ -Type Silicon Solar Cells

Je-Wei Lin, Yi-Yang Chen, Jon-Yiew Gan, Wei-Ping Hseih, Chen-Hsu Du, and Tien-Sheng Chao

**Abstract**—This research develops high open-circuit voltage ( $V_{\text{OC}}$ )  $p$ -type industrial screen-printed silicon solar cells using improved rear surface passivation. It shows a significant improvement in the minority carrier lifetime by low temperature (<450 °C) thermal atomic layer deposition of  $\text{Al}_2\text{O}_3$  layers and plasma-enhanced chemical vapor deposition of  $\text{SiN}_x$  passivation layers. An increase in the  $V_{\text{OC}}$  and the short-circuit current ( $J_{\text{SC}}$ ) due to an improved long-wavelength response are also demonstrated. With the optimized stack layers, a high efficiency of 19.2% across a large area (156  $\text{cm}^2$ ) is seen. Furthermore, the rear-side passivation scheme can be easily integrated into the conventional screen-printed process. This is very promising for in-line solar cell manufacturing.

**Index Terms**— $\text{Al}_2\text{O}_3/\text{SiN}_x$  stack layers, negative fixed charge, open-circuit voltage, surface passivation.

## I. INTRODUCTION

IN RECENT years, the importance of surface passivation to the open-circuit voltage ( $V_{\text{OC}}$ ) and cell efficiency has been well recognized. Various kinds of dielectric layers, such as silicon dioxide ( $\text{SiO}_2$ ),  $\text{SiN}_x\text{:H}$ ,  $\text{Al}_2\text{O}_3$  [1], [2], and amorphous silicon ( $\alpha\text{-Si:H}$ ) [3] have received attention due to their superior passivation ability. These layers can either chemically saturate the surface dangling bonds or offer a strong surface field. At present, the front surface passivation for a  $p$ -type substrate is optimized with  $\text{SiN}_x$  and a selective emitter (SE) structure. To further increase the efficiency, a rear-side passivation structure is crucial. To this end,  $\text{Al}_2\text{O}_3/\text{SiN}_x$  stack layers are of interest. In this approach,  $\text{Al}_2\text{O}_3$  layers deposited by atomic layer deposition (ALD) provide an excellent  $\text{Si}/\text{Al}_2\text{O}_3$  interface quality and a high negative fixed charge after annealing. In 2008, Hoex *et al.* [4] demonstrated that a satisfactorily low

density of interface defects in combination with a strong field-effect passivation is present in the  $\text{Al}_2\text{O}_3$  at the interface with the underlying Si substrate. Hoex *et al.* used both experimental and simulated data to show this, where the field-effect passivation was induced by a negative fixed charge density,  $Q_f$ , of up to  $10^{13} \text{ cm}^{-2}$ . In 2012, Vermang *et al.* [5] used a stack of  $\text{Al}_2\text{O}_3$  and  $\text{SiN}_x$  as the rear surface passivation layer. The best fill factors (FF) and short-circuit current ( $J_{\text{SC}}$ ) values were obtained by hydrophobic prepassivation cleaning and by 10 nm of  $\text{Al}_2\text{O}_3$ , in which the blistering size still increased during firing from additional outgassing. There was an apparent gain in the  $J_{\text{SC}}$  and  $V_{\text{OC}}$  due to the improved rear internal reflection and surface passivation.

This letter investigates the application of different  $\text{Al}_2\text{O}_3/\text{SiN}_x$  stack layers to passivate the rear surface of a  $p$ -type substrate using a screen-printing process. To achieve an optimized cell design, both front and rear surface conditions are varied. Six different conditions with different structures are used: 1)–3) three different homogeneous emitters ( $R_{\text{sh}} = 40$ ,  $R_{\text{sh}} = 70$ , and  $R_{\text{sh}} = 100 \text{ } \Omega/\text{sq}$ ) with a full Al back contact; 4) a SE with a full Al rear contact with sheet resistances of 40 and 100  $\Omega/\text{sq}$  for metallized and unmetallized surfaces, respectively; 5) a homogeneous emitter ( $R_{\text{sh}} = 70 \text{ } \Omega/\text{sq}$ ) with a 20/90-nm  $\text{Al}_2\text{O}_3/\text{SiN}_x$  passivated rear local back surface field (LBSF) [6]; and 6) a SE with a 20/90-nm  $\text{Al}_2\text{O}_3/\text{SiN}_x$  passivated LBSF. The improvements were applied step-by-step to demonstrate the advantages of the proposed stack layers. The characteristics of all samples, such as the saturation current density ( $J_0$ ),  $V_{\text{OC}}$ ,  $J_{\text{SC}}$ , FF, external quantum efficiency (EQE), and conversion efficiency ( $\eta$ ), are discussed and presented in this letter.

## II. EXPERIMENT

The experiments used (100)-oriented boron-doped Czochralski (Cz)  $c$ -Si square solar wafers with a thickness of 200  $\mu\text{m}$  and a resistivity of 1–2  $\Omega \text{ cm}$ . The wafers were prepared by soaking in deionized (DI) water after first performing etching of  $\sim 10 \mu\text{m}$  per side and cleaning using the standard Radio Corporation of America process. The lifetime samples had flat structures fabricated by NaOH etching and polishing. An ultrathin  $\text{SiO}_2$  layer was formed on both wafer surfaces using the nitric acid oxidation of Si method at room temperature for cleaning. The silicon surface was subsequently texturized with random pyramids in a 40-wt% KOH solution and then mixed with isopropanol and DI water at a volume ratio of 1:3:46 at 80 °C for 30 min.

Manuscript received May 14, 2013; revised June 1, 2013, June 6, 2013, and June 20, 2013; accepted June 27, 2013. Date of publication July 12, 2013; date of current version August 21, 2013. This work was supported by the Nano Facility Center of National Chiao-Tung University, the National Nano Device Laboratory, the National Science Council, Taiwan, under Contract NSC-100-2221-E-009-012-MY3, and the Green Energy and Environment Research Laboratories of the Industrial Technology Research Institute for providing the process equipment and the Bureau of Energy. The review of this letter was arranged by Editor O. Manasreh.

J.-W. Lin, W.-P. Hseih, and T.-S. Chao are with the Department of Electrophysics, National Chiao Tung University, Hsinchu 30010, Taiwan (e-mail: tschao@mail.nctu.edu.tw).

Y.-Y. Chen and J.-Y. Gan are with the Department of Materials Science and Engineering, National Tsing-Hua University, Hsinchu 30013, Taiwan.

C.-H. Du is with the Green Energy and Environment Research Labs, Industrial Technology Research Institute, Hsinchu 31040, Taiwan.

Color versions of one or more of the figures in this letter are available online at <http://ieeexplore.ieee.org>.

Digital Object Identifier 10.1109/LED.2013.2271894

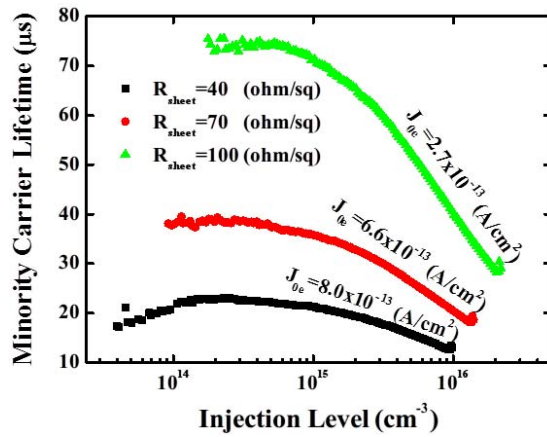


Fig. 1. Measured carrier lifetime of a 150- $\mu\text{m}$  boron-doped 1–2  $\Omega$  cm Cz Si wafer as a function of various emitter doping and excess carrier concentrations.

Front phosphorus emitters with different sheet resistances were diffused from a  $\text{POCl}_3$  source at different temperatures. The phosphorus silicate glass was removed by a short dilute HF dip. The  $\text{Al}_2\text{O}_3$  layers were deposited by thermal ALD at 200  $^\circ\text{C}$  and capped with  $\text{SiN}_x$  layers of different thicknesses by plasma-enhanced chemical vapor deposition at 450  $^\circ\text{C}$ . The samples were immersed in a nitric acid aqueous solution of 68% azeotropic concentration at room temperature for 15 min. An antireflection coating layer of  $\text{SiN}_x$  was deposited on the front side using the same conditions as the rear-side stack. The electrode was screen printed on the front and rear surfaces with silver aluminum paste. The peak temperature for cofiring was 770  $^\circ\text{C}$ . The samples were then isolated using a laser.

Characterization was performed using a Quicksun 120CA  $I$ - $V$  measurement. The photoconductivity decay (PCD) method was used to measure the lifetime and Suns  $V_{\text{OC}}$  using a Sinton Instrument WCT-120. The aperture area for all solar cells fabricated in this letter was 156  $\text{cm}^2$  and the entire front metallization, including the busbar, was contained within the active cell area. The lifetime sample structures (Figs. 1–3) are all planar.

### III. RESULTS AND DISCUSSION

The saturation current is contributed by both the emitter and LBSF regions. The front emitter is crucial to demonstrate the potential of the proposed  $\text{Al}_2\text{O}_3/\text{SiN}_x$  stack layers and requires careful optimization. The emitter quality can be classified by the emitter saturation current ( $J_{0e}$ ) and measured using the PCD method [7]. Fig. 1 shows the measured injection-dependent carrier lifetime and  $J_{0e}$  on a 150- $\mu\text{m}$  boron-doped 1–2  $\Omega$  cm Cz Si wafer with different emitter doping concentrations. The emitter doping concentration is seen to decrease (the sheet resistance rises from 40  $\Omega$  to 100  $\Omega/\text{sq}$ ). The saturation current also decreases. The optimal emitter sheet resistance for the passivated surface is 100  $\Omega$  cm and the implied  $V_{\text{OC}}$  is 650 mV. One of the difficulties in preparing a high-sheet-resistance emitter is, however, the firing conditions. Special firing processes and pastes may be required [8]. Therefore, an SE with heavily doped electrodes

TABLE I  
OVERVIEW OF THE CELL CHARACTERIZATION RESULTS (AM1.5G) WITH DIFFERENT SURFACE CONDITIONS ON  $p$ -TYPE Si SOLAR CELLS. THESE ARE OPEN-AREA EFFICIENCIES

	$V_{\text{oc}}$ [mV]	$J_{\text{sc}}$ [mA]	$P_{\text{mp}}$ [mW]	F.F. [%]	Cell eff. [%]	$R_{\text{ser}}$ [ohm-cm]
<b>Rsh 50</b>	623.6	36.2	2.82	80.0	18.1	0.18
<b>Rsh 70</b>	631.9	37.4	2.92	79.2	18.7	0.33
<b>Rsh 100</b>	626.8	37.7	2.56	69.4	16.4	2.25
<b>SE</b>	636.1	37.7	2.93	78.4	18.8	0.35
<b>LBSF</b>	640.8	37.9	2.94	77.7	18.8	0.54
<b>SE+LBSF</b>	646.3	38.0	3.00	78.2	19.2	0.66

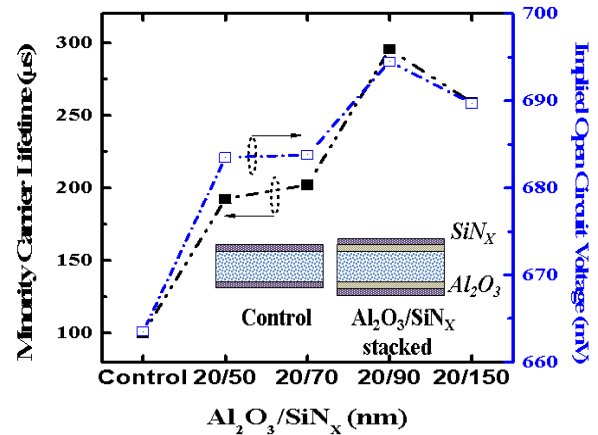


Fig. 2. Measured carrier lifetimes and implied  $V_{\text{OC}}$  of a 150- $\mu\text{m}$  boron-doped 1–2  $\Omega$  cm Cz Si wafer as a function of different  $\text{Al}_2\text{O}_3/\text{SiN}_x$  stack layers and excess carrier concentrations.

was also prepared for this purpose. The measured cell results are shown in Table I. The maximum efficiency occurs when  $R_{\text{sh}}$  is 70  $\Omega/\text{sq}$ . Although the lifetime structure shows a smaller saturation current, the nonoptimized firing, and metallization process could lead to even lower efficiency. The SE structure of the emitter has different doping concentrations under metallized and nonmetallized areas and shows improved  $V_{\text{OC}}$  and efficiency due to more tolerant firing processes. The injection-dependent lifetime of different  $\text{Al}_2\text{O}_3/\text{SiN}_x$  stack layers was also measured to determine rear-side optimization. Although the charge polarities of  $\text{SiN}_x$  and  $\text{Al}_2\text{O}_3$  are different, an effective negative charge can still be expected since the charges have varying orders between these two layers. Because of the low deposition rate,  $\text{SiN}_x$  is suitable for serving as a capping and insulating layer for  $\text{Al}_2\text{O}_3$ , where an effective negative charge can still be maintained.

Fig. 2 shows the injection-dependent lifetimes of these layer structures with various thicknesses. It can be seen that as the thickness of the  $\text{SiN}_x$  increases, the minority carrier lifetime first improves until  $\sim 150$  nm where it is seen to decay again. Although the samples were annealed at 450  $^\circ\text{C}$  before  $\text{SiN}$  deposition, extra thermal processing may still be beneficial for the charge activation. Nevertheless, extended thermal annealing may cause blistering, which degrades the

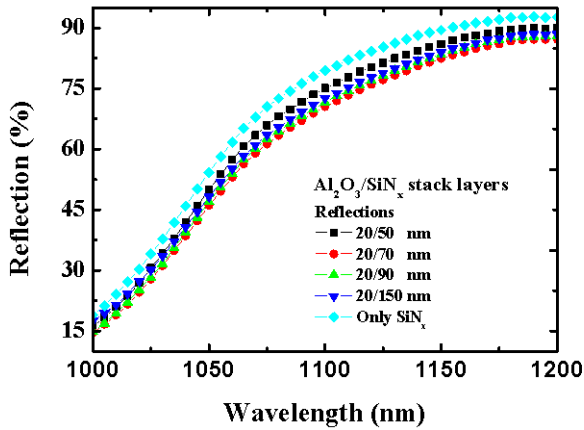


Fig. 3. Measured reflection as a function of wavelength on different  $\text{Al}_2\text{O}_3/\text{SiN}_x$  stack layer samples.

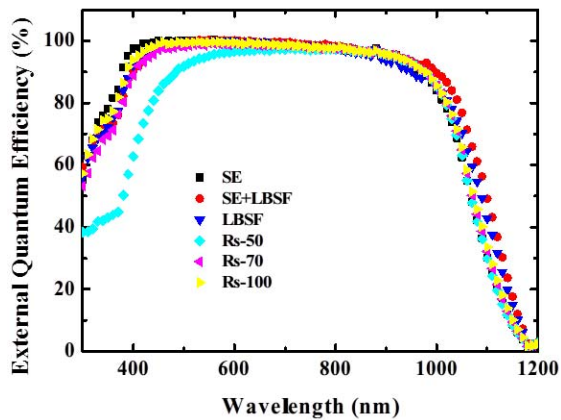


Fig. 4. Measured EQE as a function of wavelength for all split samples.

passivation when the  $\text{SiN}_x$  is too thick [9]. To optimize the rear-side reflection, the reflections with different rear-side stacks were measured and are shown in Fig. 3.

A comparison of the reflection of a single  $\text{SiN}_x$  layer and the  $\text{Al}_2\text{O}_3/\text{SiN}_x$  stack indicates that the  $\text{Al}_2\text{O}_3/\text{SiN}_x$  stack layers not only provide excellent surface passivation, but also exhibit good internal reflection. The optimized thickness is 20/70-nm  $\text{Al}_2\text{O}_3/\text{SiN}_x$ . To obtain good surface passivation and increase the  $J_{SC}$  near the long-wavelength region, 20/90-nm  $\text{Al}_2\text{O}_3/\text{SiN}_x$  stack layers were, however, studied further. Table I also shows the measured efficiency of the LBSF on the homogeneous emitter (70  $\Omega/\text{sq}$ ) and optimized front surface (the SE). Both  $J_{SC}$  and  $V_{OC}$  are improved due to better passivation and internal reflection. The FF is seen to incur a minor decrease because of the smaller contact ratio of the hole current; a significant improvement of  $\sim 0.4\%$  to 1.1% in the absolute value is obtained, if both the SE and LBSF are employed in the structure. To further demonstrate the benefits of both the SE and LBSF structures, Fig. 4 shows the measured EQE curves with the test structure used in this letter. It can be observed that the EQE in the short-wavelength

region, 300–500 nm, is remarkably enhanced with a lightly doped emitter. The Auger recombination in this region is effectively suppressed, promoting an improved blue response.

Because of the smaller absorption coefficient of long-wavelength light, the long-wavelength response is affected by the rear-side passivation and the absorption of the light. The increase of the long-wavelength response is due to improved surface passivation and higher rear internal reflection by the  $\text{Al}_2\text{O}_3/\text{SiN}_x$  stack layers, and therefore an increase in  $J_{SC}$  and  $V_{OC}$  is observed by applying the proposed stacks. Here, a high  $V_{OC}$  of 646 mV is demonstrated. The measurement of implied  $V_{OC}$ , however, still indicates a possible improvement, up to 690 mV. The limiting factor is due to the front emitter structure with an implied  $V_{OC}$  of only 660 mV. The results suggest that our proposed stack layer has great promise for application to a more advanced emitter structures.

#### IV. CONCLUSION

In this letter, the  $V_{OC}$  of an industrial screen-printed  $p$ -type Si solar cell was successfully enhanced via improved rear surface passivation using  $\text{Al}_2\text{O}_3/\text{SiN}_x$  stack layers. The carrier recombination at the surface can be effectively suppressed with a light-doped emitter of 100  $\Omega/\text{sq}$  and  $\text{Al}_2\text{O}_3/\text{SiN}_x$  stack layers. The 20/90-nm  $\text{Al}_2\text{O}_3/\text{SiN}_x$  stack layers, passivated on the rear side, not only improved the minority carrier lifetime, but also enhanced rear internal reflection. Both  $J_{SC}$  and  $V_{OC}$  were increased for silicon wafer-based solar cells. This process may be cheaper and easier to implement from an industrial standpoint.

#### REFERENCES

- [1] M. J. Kerr and A. Cuevas, "Recombination at the interface between silicon and stoichiometric plasma silicon nitride," *Semicond. Sci. Technol.*, vol. 17, no. 2, pp. 166–172, Jan. 2002.
- [2] B. Hoex, J. Schmidt, P. Pohl, *et al.*, "Silicon surface passivation by atomic layer deposited  $\text{Al}_2\text{O}_3$ ," *J. Appl. Phys.*, vol. 104, no. 4, pp. 044903-1–044903-12, Aug. 2008.
- [3] S. Olibet, E. Vallat-Sauvain, and C. Ballif, "Model for a-Si:H/c-Si interface recombination based on the amphoteric nature of silicon dangling bonds," *Phys. Rev. B, Condens. Matter*, vol. 76, no. 3, p. 035326, Jul. 2007.
- [4] B. Hoex, J. J. H. Gielis, M. C. M. van de Sanden, *et al.*, "On the c-Si surface passivation mechanism by the negative-charge-dielectric  $\text{Al}_2\text{O}_3$ ," *J. Appl. Phys.*, vol. 104, no. 11, pp. 113703-1–113703-7, Dec. 2008.
- [5] B. Vermang, H. Goverde, A. Uruena, *et al.*, "Blistering in ALD  $\text{Al}_2\text{O}_3$  passivation layers as rear contacting for local Al BSF Si solar cells," *Solar Energy Mater. Solar Cells*, vol. 101, pp. 204–209, Jun. 2012.
- [6] S. Ramanathan, A. Das, B. I. Cooper, *et al.*, "20% efficient screen printed LBSF cell fabricated using UV laser for rear dielectric revoal," in *Proc. 35th IEEE PVSC*, Jun. 2010, pp. 678–682.
- [7] M. Kerr, "Surface, emitter and bulk recombination in silicon and development of silicon nitride passivated solar cells," Ph.D. dissertation, Dept. Eng., Australian Nat. Univ., Canberra, Australia, Jun. 2002.
- [8] B. Raabe, F. Book, A. Dastgheib-Shirazi, *et al.*, "The development of etch-back processes for industrial silicon solar cells," in *Proc. 25th Eur. Photovolt. Solar Energy Convers.*, Sep. 2010, pp. 1174–1178.
- [9] B. Vermang, H. Goverde, L. Tous, *et al.*, "Approach for  $\text{Al}_2\text{O}_3$  rear surface passivation of industrial p-type Si PERC above 19%," *Prog. Photovolt. Res. Appl.*, vol. 20, no. 3, pp. 269–273, May 2012.